Nonlinear Dynamics and Systems Theory, **25** (1) (2025) 1–12

The Dynamics and Stability of Prey-Predator Model of Migration with Holling Type-III Response Function and Interspecific Competition for Prey

Syamsul Agus, Syamsuddin Toaha *, Kasbawati and Khaeruddin

Department of Mathematics, Hasanuddin University, Tamalanrea, 90245, Makassar, Indonesia

Received: April 30, 2024; Revised: January 11, 2025

Abstract: This paper discusses the prey-predator model with habitats in reserved and unreserved areas. The prey population can migrate from the reserved area to the unreserved area and vice versa. The prey lives in the reserved and unreserved areas. The predator freely hunts for the prey in the unreserved area. The Holling type III is considered on the basis of its predatory characteristics. Interspecific competition for prey occurs in the migration process. The dynamics of prey-predator is expressed as a system of nonlinear differential equations. The stability of the interior equilibrium point is analyzed locally. The eigenvalues of the Jacobian matrix together with the Routh-Hurwitz stability test are used to determine the stability of the equilibrium point. Using appropriate parameter values, simulations were conducted by varying the parameter values of migration and interspecific competition. It was found that there are up to three interior equilibrium points and there are conditions in which there is no interior equilibrium point. It was also found that there are three interior equilibrium points, one of which is unstable while the other two are bistable. The change in migration rates and competition levels allows the prey population in the reserved and unreserved areas and their predator to live together.

Keywords: *prey-predator; Holling type; reserved area; interspecific competition; bistable equilibrium points.*

Mathematics Subject Classification (2020): 70K42, 70K20, 93D05.

* Corresponding author: mailto::syamsuddint@gmail.com

1 Introduction

A mangrove forest is an ecosystem developed between estuaries and coastal areas. Mangrove ecosystems are migration routes for many species of fish and other organisms. Mangrove forests are the habitat of many species, including mangrove crabs, for feeding, breeding, and protection from predators. In their life cycle, juvenile crabs migrate back to the estuary, gradually enter the mangrove area, and develop into adults [1]. Mangrove crabs are species that tend to attack and eat other mangrove crabs. Around mangrove forests and coastal areas, the crab is preyed on by many fish, including Red Snapper (*Lutjanidae*) and White Snapper (*Lates calcarifer*). In addition, various types of fish dominated by carnivorous fish approach mangrove forests at high tide to find food [2]. The dynamics of population changes of migrating mangrove crabs and their predators can be expressed in the form of a mathematical model.

The population dynamics dealing with the prey-predator model has been studied by many researchers from different angles and with different purposes. Some researchers focus on the effect of predation functions such as the Holling function and the Beddington-DeAngelis function, which consider the characteristics of predators in hunting to catch their prey, see for example, [3–5]. Population dynamics in ecology also includes many prey-predator interactions, harvesting and its consequences in the population dynamics mechanism [6]. For certain reasons and conditions, the habitat of a population is divided into a reserved area and an unreserved area for economic activities. Under such conditions, the population is divided based on where it is located and the population can still migrate from the reserved area to the unreserved area and vice versa [7, 8]. Migration and harvesting in a prey-predator model can also be used as a control in bio-economic models and an effort to prevent the population from extinction and to optimally utilize the population as a valuable stock [9, 10].

Based on the previous research, a prey-predator model with prey migration in the two areas and interspecific competition was developed. In this model, the influences of migration and interspecific competition on the stability of the equilibrium point and sustainability of the populations are analyzed. Mangrove crabs as the prey migrate from mangrove area to the coastal area and vice versa, with mangroves as a reserved area and the coastal zone as an unreserved area. Predator populations freely prey on mangrove crabs in the unreserved area and follow the Holling type III predation function according to the characteristics of populations. In the process of migration, interspecific competition between prey occurs naturally. The dynamics of prey and predator populations is expressed as a system of nonlinear differential equations. The population dynamics is analyzed by checking the conditions for the existence of interior equilibrium points and analyzing the local stability. The nonlinear model is complex enough to be solved analytically. The Routh-Hurwitz stability test is used to investigate the local stability of the interior equilibrium point of the model. The effects of migration rate and interspecific competition on prey are analyzed using numerical simulations. The plots of trajectory curves for prey and predator populations around the stable interior equilibrium point are given to visualize the dynamics of prey and predator populations.

2 Methodology of Prey-Predator Model with Migration

This paper considers the dynamics of mangrove crabs or mud crabs (*Scylla spp.*) living in the mangrove area and in marine waters. Mangrove crabs mate in the mangrove area

and migrate to marine waters to spawn. After spawning and growing into juvenile crabs, they migrate back to the upstream estuary or back to the mangrove area. When the mangrove crabs are in the mangrove area, they are relatively safe from predators, but in the marine waters, a certain fish as a predator will prey on the mangrove crabs. In this case, the mangrove crab habitat is divided into two parts, namely the mangrove area as the reserved area and the marine waters as the unreserved area. In the migration process of mangrove crabs, interspecific competition occurs and reduces the number of mangrove crabs [4, 11]. The mangrove crabs living in the mangrove area and marine waters are assumed to grow according to the logistic model. Predation on the mangrove crabs occurs only in the unreserved area and the predation function follows the Holling type III, which is consistent with the characteristics of predation on crabs [4]. In the predator populations, intraspecific competition occurs [12] and the prey and predator populations are reduced by natural mortality.

The population dynamics of mangrove crabs in the reserved and unreserved areas and of their predator are expressed in the following growth model:

$$\begin{aligned} \frac{dx}{dt} &= rx(1-\frac{x}{K}) - \sigma_1 x + \sigma_2 y - \frac{cx^2 z}{c_1 + x^2} - fx - uxy, \\ \frac{dy}{dt} &= sy(1-\frac{y}{L}) + \sigma_1 x - \sigma_2 y - hy - vxy, \\ \frac{dz}{dt} &= \frac{g_1 x^2 z}{c_1 + x^2} - ez - qz^2. \end{aligned} \tag{1}$$

In model (1), the variables $x = x(t)$, and $y = y(t)$ are the population densities of mangrove crab as prey in the unreserved and reserved areas at time t, respectively. The variable $z = z(t)$ is the population density of fish as the predator at time t. The initial conditions of all three populations are nonnegative, $x\,(0) \geq 0$, $y\,(0) \geq 0$, and $z\,(0) \geq 0$. Parameters $r, K, \sigma_1, \sigma_2, c, c_1, f, h, e, s, L, g_1, q, u,$ and v successively express the intrinsic growth rate of the prey population in the unreserved area, the carrying capacity of the habitat for the prey population in the unreserved area, the weighting coefficient of prey migration from the unreserved area to the reserved area, the weighting coefficient of prey migration from the reserved area to the unreserved area, the maximum per capita consumption rate of the predator, the Michaelis-Menten constant rate, prey mortality rate in the unreserved area, prey mortality rate in the reserved area, predator mortality rate, intrinsic growth rate of the prey population in the reserved area, carrying capacity of the habitat for the prey population in the reserved area, conservation rate of predator, intraspecific competition coefficient, prey competition in the reserved area, and prey competition in the unreserved area. All parameters are assumed to be positive.

For simplicity, let $R = r - \sigma_1 - f$, $R_1 = \frac{r}{K}$, $S = s - \sigma_2 - h$, $S_1 = \frac{s}{L}$, $\gamma = \frac{g_1 - e}{q}$, $\gamma_1 = \frac{ec_1}{q}$. Furthermore, model (1) is expressed as

$$\frac{dx}{dt} = x[(R - R_1 x) - \frac{cx^2 z}{c_1 + x^2} - uy] + \sigma_2 y, \tag{2}$$

$$\frac{dy}{dt} = y[(S - S_1 y) - vx] + \sigma_1 x, \tag{3}$$

$$\frac{dz}{dt} = z(\frac{g_1 x^2}{c_1 + x^2} - e - q_3 z). \tag{4}$$

3 Positivity and Boundedness of Solution

The positivity and boundedness of the solution of model (1) with the initial conditions $x(0) > 0, y(0) > 0, z(0) > 0$ are stated in the form of theorems. The positivity and boundedness of the solution of the model are ecologically relevant.

Theorem 3.1 *The set* $\Psi = \left\{(x,\ y,\ z) \in \Re^3_{+0} : 0 < \omega = x + y + z \leq \frac{\rho}{\rho_1}\right\}$ *is the area for all solutions of the subsets in the positive octant, where* ρ_1 *is a constant which satisfies* $\rho_1 < e, \rho = \frac{K(r-f+\rho_1)^2}{4r} + \frac{L(s-h+\rho_1)^2}{4s}, g_1 \leq c.$

Proof. Let $\omega(t) = x(t) + y(t) + z(t)$ and $\rho_1 > 0$ be a constant. Then $\frac{d\omega}{dt} + \rho_1\omega = (r - f + \rho_1)x - \frac{rx^2}{K} - (u + v)xy + (s - h + \rho_1)y - \frac{sy^2}{L} - (c - g_1)\frac{x^2z}{c_1+x^2} - (e - \rho_1)z - qz^2$. It is natural to assume that $g_1 \leq c$, so the equation can be written as

$\frac{d\omega}{dt} + \rho_1\omega = -\frac{r}{K}(x - \frac{K}{2r}(r - f + \rho_1))^2 - \frac{s}{L}(y - \frac{L}{2s}(s - h + \rho_1))^2 + \frac{K}{4r}(r - f + \rho_1)^2 + \frac{L}{4s}(s - h + \rho_1)^2 - (u + v)xy - (c - g_1)\frac{x^2z}{c_1+x^2} - (e - \rho_1)z - qz^2.$

$\frac{d\omega}{dt} + \rho_1\omega \leq \frac{K}{4r}(r - f + \rho_1)^2 + \frac{L}{4s}(s - h + \rho_1)^2 = \rho.$

By the theory of differential inequalities, we have $0 < \omega(x(t), y(t), z(t)) \leq \frac{\rho}{\rho_1}(1 - \frac{1}{e^{\rho_1 t}}) + \omega(x(t), y(t), z(t))\frac{1}{e^{\rho_1 t}}$. Taking limit when $t \to \infty$, we get $0 < \omega \leq \frac{\rho}{\rho_1}$. This proves the theorem.

Theorem 3.2 *All solutions* $(x(t), y(t), z(t))$ *of the system of equations (2), (3), and (4) with the initial conditions* $x(0) > 0, y(0) > 0, z(0) > 0$ *are positive for all* $t \geq 0$.

Proof. From equation (2) together with the initial conditions $x(0) > 0, y(0) > 0, z(0) > 0$, we have $\frac{dx}{x} = \mu(x, y, z)dt + \mu_1(x, y)dt$, where $\mu(x, y, z) = (R - R_1x) - \frac{cxz}{c_1+x^2} - uy$, and $\mu_1(x, y) = \frac{\sigma_2 y}{x}$. Integrating the above equation on the interval $\lfloor 0, \tau \rfloor$, we have $x(t) = x(0)e^{\int_0^t \mu(x(\tau),y(\tau),z(\tau))d\tau + \int_0^t \mu_1(x(\tau),\ y(\tau))d\tau} > 0$ for all $\tau \in [0,\ t]$.

Next, from equation (3), we have $\frac{dy}{y} = \varphi_0(x, y)\, dt + \varphi_1(x,\ y)\, dt$, where $\varphi_0(x, y) = (S - S_1y) - vx,\ \varphi_1(x,\ y) = \frac{\sigma_1 x}{y}$. Integrating the above equation on the interval $\lfloor 0, \tau \rfloor$, we have $y(t) = y(0)e^{\int_0^t \varphi_0(x(\tau),y(\tau))d\tau + \int_0^t \varphi_1(x(\tau),y(\tau))d\tau} > 0$ for all $\tau \in [0,\ t]$.

Next, from equation (4), we have $\frac{dz}{z} = \rho_0(x, z)\, dt$, where $\rho_0(x, z) = \frac{g_1x^2}{c_1+x^2} - e - qz$. Integrating the above equation on the interval $\lfloor 0, \tau \rfloor$, we have $z(t) = z(0)e^{\int_0^t \rho_0(x(\tau),z(\tau))d\tau} > 0$ for all $\tau \in [0,\ t]$. The solutions of the equations (2), (3), and (4) are all positive.

Theorem 3.3 *All solutions of the model (1) are bounded.*

Proof. We construct a function $\omega(t) = x(t) + y(t) + \frac{c}{g_1}z(t)$. If this equation is differentiated with respect to time (t), then we have $\frac{d\omega}{dt} = rx\left(1 - \frac{x}{K}\right) - fx - (u + v)xy + sy\left(1 - \frac{y}{L}\right) - hy - \frac{ec}{g_1}z - \frac{q_3c}{g_1}z^2$,

$\frac{d\omega}{dt} = rx + ex - \frac{rx^2}{K} - fx - (u + v)xy + sy + ey - \frac{sy^2}{L} - hy - \frac{ec}{g_1}z - \frac{q_3c}{g_1}z^2 - ex - ey,$

$\frac{d\omega}{dt} \leq rx + ex + sy + ey - \frac{ec}{g_1}z - ex - ey.$

The consumption rate of the predator population to prey is assumed to follow $0 < g_1 \leq c$. From the first two equations of model (1), we have $K + L$ is the total carrying capacity of the total prey population. We have $x(t) + y(t) \leq K + L + \epsilon$ as $t \to \infty$. Suppose we take $x(t) \leq K + \epsilon_1$ as $t \to \infty$ and $y(t) \leq L + \epsilon_2$ as $t \to \infty$, where $\epsilon,\ \epsilon_1,\ \epsilon_2$ are three positive numbers. Let $\omega(t) = x(t) + y(t) + \frac{c}{g_1}z$. The derivative of

$\omega(t)$ with respect to t takes the form

$$\begin{aligned}\frac{d\omega}{dt} &\leq (r+e)\,x + (s+e)\,y - \frac{ec}{g_1}z - ex - ey\\ &= -e\left(x + y + \frac{c}{g_1}z\right) + (e+r)\,x + (e+s)\,y\\ &= -e\omega + (e+r)\,x + (e+s)\,y,\\ \frac{d\omega}{dt} + e\omega &\leq (e+r)\,(K+\epsilon_1) + (e+s)\,(L+\epsilon_2).\end{aligned}$$

Let $K_1 = (e+r)\,(K+\epsilon_1) + (e+s)\,(L+\epsilon_2)$ and integrate both sides, we obtain the boundary $\omega(t) = \frac{K_1}{e} + C_1\,\frac{1}{e^{et}}$. The inequality $\frac{d\omega}{dt} \leq K_1 - e\omega$ has the solution $\omega(t) \leq \frac{K_1}{e} + C_1\,\frac{1}{e^{et}}$ for $t \to \infty$. Then we obtain $\limsup_{t\to\infty}\omega(t) \leq \frac{K_1}{e}$. Therefore, (x, y, z) is bounded in $\mathfrak{R}^3$ and (x, y, z) belongs to $\Psi_1 = \left\{(x,\ y,\ z) \in \mathfrak{R}^3_{+0} : x + y + \frac{ec}{g_1}z \leq \frac{K_1}{e}\right\}$.

4 Equilibrium Points and Local Stability Analysis

In order to investigate the behavior and changes of the populations x, y, and z, it is necessary to find the interior equilibrium point and determine its stability. The equilibrium points of model (1) are obtained by solving $\frac{dx}{dt} = \frac{dy}{dt} = \frac{dz}{dt} = 0$. Further, the non-negative equilibrium points are obtained, namely $T_1 = (0, 0, 0)$ and $T_2 = (x_2, y_2, 0)$. The values of components of the equilibrium point T_2 are $x_2 = \frac{y_2(-y_2S_1+S)}{vy_2-\sigma_1}$ and y_2, where y_2 is the positive root of the polynomial $AX^3 + BX^2 + CX + D = 0$, where $A = R_1{S_1}^2 - uvS_1$, $B = RvS_1 - 2SS_1R_1 + Suv + uS_1\sigma_1 - \sigma_2v^2, C = S^2R_1 - RSv - RS_1\sigma_1 - Su\sigma_1 + 2\sigma_1\sigma_2v$, and $D = RS\sigma_1 - \sigma_2{\sigma_1}^2$. The possible interior equilibrium point for model (1) is $T_3 = (\bar{x},\ \bar{y},\ \bar{z})$. The values of components of the equilibrium point T_3 are $\bar{x} = \frac{\bar{y}(-\bar{y}S_1+S)}{v\bar{y}-\sigma_1}$, $\bar{z} = \frac{\gamma\bar{x}^2-\gamma_1}{\bar{x}^2+c_1}$, and $\bar{y}$, where $\bar{y}$ is the positive root of the polynomial $A_1Y^{11} + A_2Y^{10} + A_3Y^9 + A_4Y^8 + A_5Y^7 + A_6Y^6 + A_7Y^5 + A_8Y^4 + A_9Y^3 + A_{10}Y^2 + A_{11}Y + A_{12} = 0$, where A_1, A_2, ..., A_{12} are real numbers that depend on the values of the model parameters.

The equilibrium point $T_3 = (\bar{x},\ \bar{y},\ \bar{z})$ may not exist in the sense that not all of its components are positive. The equilibrium point $T_3 = (\bar{x},\ \bar{y},\ \bar{z})$ may consist of only one, two, three or more components in the first octant. This condition depends on the parameter values of the model. The only equilibrium point to be analyzed is the interior equilibrium point, i.e., $T_3 = (\bar{x},\ \bar{y},\ \bar{z})$. Due to the complexity of model (1), only the local stability of the interior equilibrium point is considered. For this purpose, the model is linearized around the equilibrium point and the Jacobian matrix evaluated at the equilibrium point $T_3 = (\bar{x},\ \bar{y},\ \bar{z})$ is obtained as follows:

$$J(T_3) = \begin{pmatrix} d_1 & d_2 & d_3\\ d_4 & d_5 & 0\\ d_6 & 0 & d_7\end{pmatrix},$$

where $d_1 = R - 2R_1\bar{x} - \frac{2c\bar{x}\bar{z}}{\bar{x}^2+c_1} - u\bar{y} + \frac{2c\bar{x}^3\bar{z}}{(\bar{x}^2+c_1)^2}$, $d_2 = \sigma_2 - u\bar{x}$, $d_3 = -\frac{c\bar{x}^2}{\bar{x}^2+c_1}$, $d_4 = \sigma_1 - v\ \bar{y}, d_5 = S - v\bar{x} - 2\bar{y}S_1$, $d_6 = \frac{2g_1c_1\bar{x}\bar{z}}{(\bar{x}^2+c_1)^2}$, and $d_7 = \frac{g_1\bar{x}^2}{\bar{x}^2+c_1} - e - 2q\bar{z}$.

The next step is obtaining the characteristic equation that corresponds to the equilibrium point $T_3 = (\bar{x},\ \bar{y},\ \bar{z})$. Then we have $f(\lambda) = \lambda^3 + a_1\lambda^2 + a_2\lambda + a_3$, where $a_1 =$

$-(d_1+d_5+d_7)$, $a_2 = d_1d_5+d_5d_7+d_1d_7-d_2d_4-d_3d_6$, and $a_3 = d_2d_4d_7-d_1d_5d_7+d_3d_5d_6$. In accordance with the Routh-Hurwitz stability test [13], the interior equilibrium point $T_3 = (\bar{x},\ \bar{y},\ \bar{z})$ is locally asymptotically stable if the conditions $a_1 > 0, a_3 > 0$, and $a_1a_2 - a_3 > 0$ are satisfied.

5 Numerical Simulation

The simulation is based on the analysis results obtained in the previous section. Simulations are performed to investigate the effect of migration and interspecific competition in the prey population on the existence of interior equilibrium points in the first octant and their stability. The parameter values used in the simulation of model (1) are based on the parameter values used by the previous researchers [6, 14, 15]. Some parameter values have been adjusted to get interesting results. The values of migration rates and interspecific competition are given in various combinations. The simulation is given in four cases, which are presented in the table and plot of prey and predator population curves in the reserved and unreserved areas.

Case 1. The value of σ_1 is fixed and the value of σ_2 varies.

For simulation, we use the parameter values $r = 0.9, K = 100, L = 100, c = 2.5, g_1 = 0.8, c_1 = 1, f = 0.02, h = 0.01, e = 0.3, q = 0.3, u = 0.02$, and $v = 0.02$ in the appropriate units. By using these parameter values, the equilibrium points, eigenvalues, and stability are obtained, as shown in Table 1.

$\sigma_2 = 0.1$	$\sigma_2 = 0.2$	$\sigma_2 = 0.4$	$\sigma_2 = 0.5$
$T_{3a}(7.66, 1.02, 1.62)$ (0.52,-0.87,-0.48) not stable	$T_{3a}(7.18, 0.95, 1.62)$ (0.51,-0.85,-0.47) not stable	$T_{3a}(6.39, 0.80, 1.60)$ (0.49,-0.84,-0.46) not stable	$T_{3a}(6.08, 0.73, 1.60)$ (0.49,-0.86,-0.45) not stable
	$T_{3b}(1.02, 54.01, 0.37)$ (-10.48,-0.13,-0.48) stable node	$T_{3b}(1.80, 15.63, 1.04)$ (-2.72,-0.45,-0.18) stable node	$T_{3b}(1.88, 5.40, 1.08)$ (-0.55±0.58i,-0.14) stable node
$T_{3c}(68.18, 0.53, 1.67)$ (-0.55,-12.86,-0.50) stable node	$T_{3c}(68.37, 0.53, 1.67)$ (-0.55,-12.99,-0.50) stable node	$T_{3c}(68.75, 0.52, 1.67)$ (-0.56,-13.27,-0.50) stable node	$T_{3c}(68.9, 0.51, 1.67)$ (-0.56,-13.41,-0.50) stable node

Table 1: The equilibrium point T_3, eigenvalues, and stability for the case $\sigma_1 = 0.1$.

Table 1 shows that there are initially two equilibrium points in the first octant, one equilibrium point is unstable and the other is locally asymptotically stable. By increasing the value of the migration coefficient (σ_2) from the reserved to the unreserved area, three equilibrium points are obtained in the first octant, where one equilibrium point remains unstable while the other two are locally asymptotically stable. In this case, there is a bistable equilibrium point, i.e., the coexistence of two equilibrium points that are jointly stable, and the type of stability is the same, i.e., they are locally asymptotically stable with node type. By increasing the value of the migration coefficient (σ_2), three equilibrium points are still obtained in the first octant and their stability does not change.

Increasing the value of σ_2 only changes the value of the equilibrium point T_{3a}, i.e., the values of the equilibrium points of the populations x, y, and z are all decreasing. The equilibrium point T_{3b} does not appear at first. By increasing the value of σ_2, the equilibrium point T_{3b} appears, and the increase in the value of σ_2 changes the values of the equilibrium points T_{3b} and T_{3c}; that is, the values of the equilibrium points of the populations x and z increase while the value of the equilibrium point of the population y decreases.

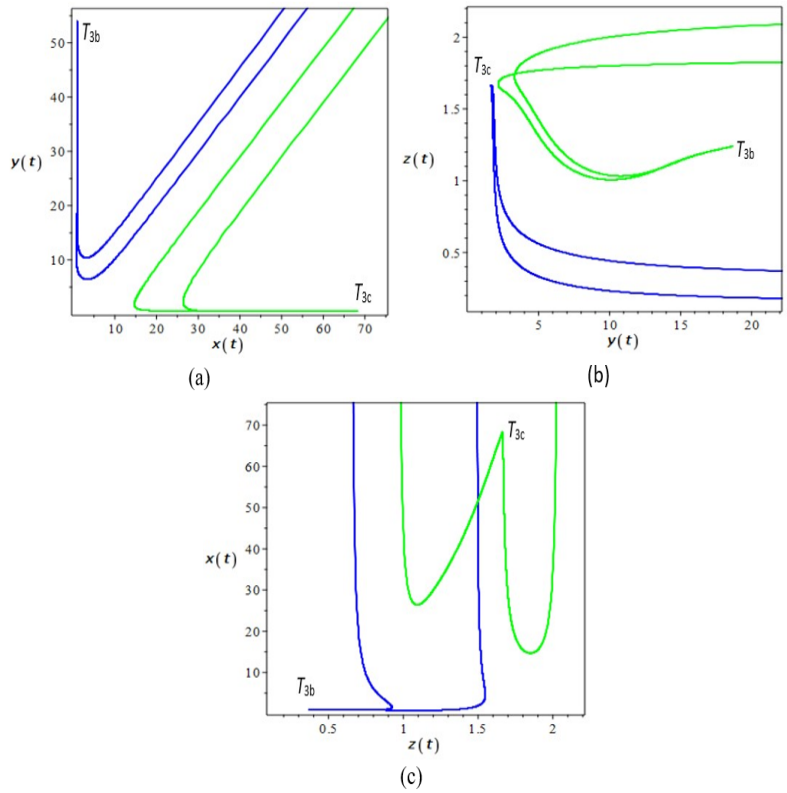

Figure 1: Populations behaviour around the bistable equilibrium points for $\sigma_1 = 0.1, \sigma_2 = 0.2$.

Figure 1 shows the behaviour of the populations x, y and z around the two stable equilibrium points. Both equilibrium points T_{3b} and T_{3c} are asymptotically stable, i.e., they are bistable equilibrium points. This means that none of the three populations will become extinct. The initial value of the population plays an important role in determining where the population converges. In Figure 1(a), there is a line dividing the stability domain for the equilibrium points T_{3b} and T_{3c}, but in Figures 1(b) and 1(c), the line which divides the stability domain for the equilibrium points T_{3b} and T_{3c} is not clearly visible.

Case 2. The value of σ_2 is fixed and the value of σ_1 varies.

For simulation, we use the parameter values $r = 0.9, K = 100, L = 100, c = 2.5, g_1 =$

$0.8, c_1 = 1, f = 0.02, h = 0.01, e = 0.3, q = 0.3, u = 0.02$, and $v = 0.02$ in the appropriate units. By using these parameter values, the equilibrium points, eigenvalues, and stability are obtained, as shown in Table 2.

$\sigma_1 = 0.05$	$\sigma_1 = 0.1$	$\sigma_1 = 0.2$	$\sigma_1 = 0.25$
$T_{3a}(6.02, 0.72, 1.60)$ (-0.45±0.03i,0.62) not stable, spiral	$T_{3a}(7.66, 1.02, 1.62)$ (0.52,-0.87,-0.48) not stable	$T_{3a}(14.39, 1.37, 1.66)$ (0.23,-2.20,-0.49) not stable	T_{3a} does not appear
$T_{3b}(80.68, 0.26, 1.67)$ (-0.67,-15.35,-0.50) stable node	$T_{3b}(68.18, 0.53, 1.67)$ (-0.55,-12.86,-0.50) stable node	$T_{3b}(39.52, 1.11, 1.67)$ (-0.23,-7.16,-0.50) stable node	T_{3b} does not appear

Table 2: The equilibrium point T_3, eigenvalues, and stability for the case $\sigma_2 = 0.1$.

There are two equilibrium points in the first octant, as Table 2 demonstrates. At first, one equilibrium point exhibits spiral stability, while the other displays local asymptotic stability. By increasing the value of the migration coefficient (σ_1) from the unreserved to the reserved area, two equilibrium points are still obtained in the first octant, but the spiral unstable equilibrium point becomes an unstable node and the other equilibrium point remains locally asymptotically stable. When increasing the value of σ_1 again, there are still two equilibrium points with the type of stability unchanged. However, when $\sigma_1 = 0.25$, the equilibrium point in the first octant is no longer obtained. The increase of the migration value from the unreserved to the reserved area can lead to the non-existence of the equilibrium point in the first octant.

Case 3. The value of u is fixed and the value of v varies.

For simulation, we use the parameter values $r = 0.9, K = 100, L = 100, c = 2.5, g_1 = 0.8, c_1 = 1, f = 0.02, h = 0.01, e = 0.3, q = 0.3, \sigma_1 = 0.3$, and $\sigma_2 = 0.3$ in the appropriate units. By using these parameter values, the equilibrium points, eigenvalues, and stability are obtained, as shown in Table 3.

$v = 0.1$	$v = 0.2$	$v = 0.4$	$v = 0.5$
	$T_{3a}(13.04, 1.92, 1.65)$ (0.18,-2.09,-0.49) not stable	$T_{3a}(9.26, 0.89, 1.63)$ (0.31,-3.14,-0.48) not stable	$T_{3a}(8.87, 0.69, 1.63)$ (0.33,-3.86,-0.48) not stable
$T_{3b}(2.63, 38.6, 1.33)$ (-3.51,-0.49,-0.38) stable node	$T_{3b}(2.29, 18.79, 1.24)$ (-1.00±0.02i,-0.27) stable spiral	$T_{3b}(1.58, 5.17, 0.91)$ (-0.38±0.74i,-0.38) stable spiral	$T_{3b}(1.41, 3.02, 0.77)$ (-0.28±0.71i,-0.19) stable spiral
	$T_{3c}(34.42, 1.64, 1.66)$ (-0.19,-6.34,-0.49) stable node	$T_{3c}(46.44, 0.77, 1.66)$ (-0.33,-18.00,-0.49) stable node	$T_{3c}(48.5, 0.61, 1.66)$ (-0.35,-23.67,-0.50) stable node

Table 3: The equilibrium point T_3, eigenvalues, and stability for the case $u = 0.1$.

Table 3 shows that initially there is only one equilibrium point in the first octant, which is locally asymptotically stable. When increasing the value of the competition coefficient in the population y, three equilibrium points appear in the first octant, one equilibrium point is unstable, while the other two are spiral stable and nodal stable. If we increase the value of the competition coefficient in the population y again, we find that there are still three equilibrium points in the first octant, and their stability does not change. Increasing the competition coefficient only affects the value of the equilibrium points. For the equilibrium points T_{3a} and T_{3b}, increasing the competition coefficient decreases the values of the equilibrium points for the populations x, y, and z. While for the equilibrium point T_{3c}, the values of the equilibrium point for the population y decreases, but the values of the equilibrium points for the populations x and z increase.

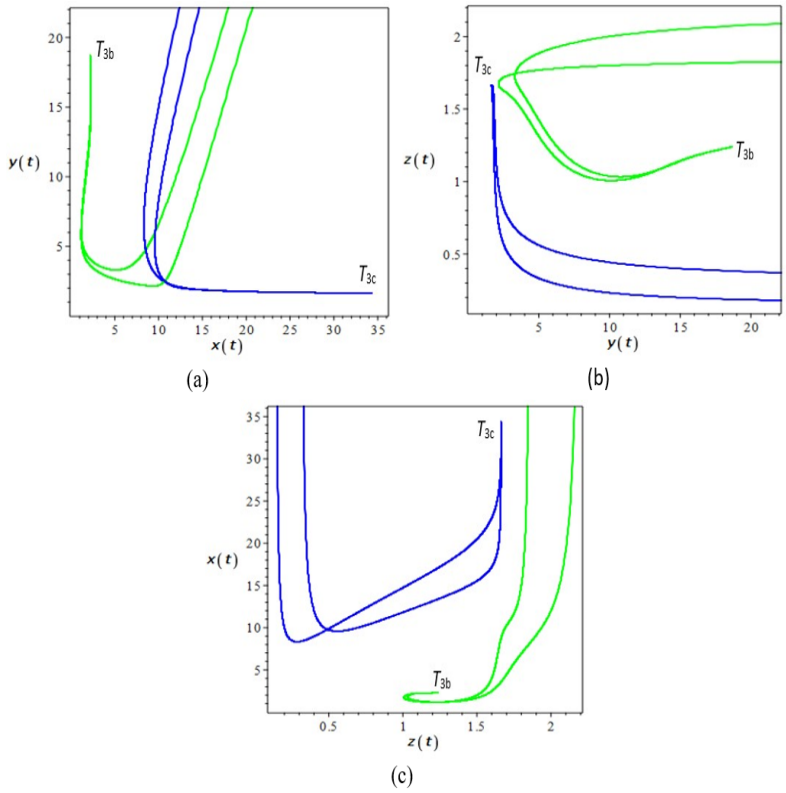

Figure 2: Populations behaviour around the bistable equilibrium points for $u = 0.1, v = 0.2$.

Figure 2 shows the behaviour of the populations x, y, and z around two stable equilibrium points. Both equilibrium points T_{3b} and T_{3c} are asymptotically stable, bistable equilibrium points. This means that none of the three populations will become extinct. The initial value of the population determines to what interior equilibrium point the population converges. In Figure 2(a), there is no clear curve that divides the domain of stability for the equilibrium points T_{3b} and T_{3c}, but in Figures 2(b) and 2(c), there is a clear curve that divides the domain of stability for the equilibrium points T_{3b} and T_{3c}.

Case 4. The value of v is fixed and the value of u varies.

For simulation, we use the parameter values $r = 0.9, K = 100, L = 100, c = 2.5, g_1 = 0.8, c_1 = 1, f = 0.02, h = 0.01, e = 0.3, q = 0.3, \sigma_1 = 0.3$, and $\sigma_2 = 0.3$ in the appropriate units. By using these parameter values, the equilibrium points, eigenvalues, and stability are obtained as shown in Table 4.

$u = 0.1$	$u = 0.2$	$u = 0.3$	$u = 0.4$
$T_{3a}(13.04, 1.92, 1.65)$ (0.18,-2.09,-0.49) not stable			
$T_{3b}(2.29, 18.79, 1.24)$ (-1.00±0.02i,-0.27) stable spiral	$T_{3b}(1.43, 35.19, 0.79)$ (-7.03,-0.35,-0.27) stable node	$T_{3b}(1.01, 43.87, 0.35)$ (-13.02,-0.12,-0.40) stable node	T_{3b} does not appear, z becomes negative
$T_{3c}(34.42, 1.64, 1.66)$ (-0.19,-6.34,-0.49) stable node			

Table 4: The equilibrium point T_3, eigenvalues, and stability for the case $v = 0.2$.

Table 4 shows that there are initially three equilibrium points in the first octant, i.e., the equilibrium point T_{3a} is unstable, while the equilibrium points T_{3b} and T_{3c} are spiral stable and node stable, respectively. By increasing the value of the competition coefficient (u), only one unstable node equilibrium point is obtained. However, for the competition coefficient $u = 0.4$, there is no equilibrium point in the first octant. Increasing the value of the competition coefficient can lead from three equilibrium points to only one node-stable equilibrium point, and then no more equilibrium points exist in the first octant.

6 Conclusion

The population dynamics of prey living in the reserved and unreserved areas and of their predators living in the unreserved areas are expressed by a system of nonlinear differential equations. This model can describe the population dynamics of mangrove crabs living in mangrove forests and the coastal area. Mangrove crabs in the coastal area are preyed upon by predatory fish that follow the Holling type III predation function. The solution of the model is positive and bounded in the first octant. Simulations with the relevant values of the model parameters have found one, two, three, and even no interior equilibrium points. Some of these interior equilibrium points are stable, and some are unstable.

Simulations were carried out by changing the value of the migration rates in the prey population living in the reserved and unreserved areas. In case 1, initially, only two interior equilibrium points were found, one stable and the other unstable. Once the value of the migration rate σ_2 is increased and three equilibrium points are obtained, one equilibrium point is unstable and the other two equilibrium points are stable; bistable equilibrium points occur. In case 2, two interior equilibrium points are initially obtained,

one equilibrium point is stable and the other is unstable. By increasing the migration rate (σ_1), two interior equilibrium points are still obtained, but there is a change in the type of stability, from unstable spiral to unstable saddle. By increasing the migration rate (σ_1) again, the interior equilibrium point is no longer found.

Simulations were also conducted by changing the level of competition in the prey population. In case 3, initially, there is only one stable interior equilibrium point. Once the competition level (v) is increased, three equilibrium points are obtained: one equilibrium point is unstable, and the other two equilibrium points are stable, stable node and stable spiral. In this case, there are bistable equilibrium points. In case 4, initially, three interior equilibrium points are obtained, two equilibrium points are stable, stable node and stable spiral, and the other one is unstable. By increasing the competition level (u), only one stable node interior equilibrium point is obtained. By increasing the competition level (u) again, the interior equilibrium point is no longer found.

References

[1] L. Le Vay. Ecology and management of mud crab Scylla spp. *Asian Fisheries Science* **14** (2) (2001) 101–112.

[2] I. Nagelkerken, S. J. M. Blaber, S. Bouillon, P. Green, M. Haywood, L. G. Kirton and J. O. Meynecke *et al.* The habitat function of mangroves for terrestrial and marine fauna: A Review. *Aquatic Botany* **89** (2) (2008) 155–185.

[3] Noor S. Sh. Barhoom, and S. Al-Nassir. Dynamical behaviors of a fractional-order three-dimensional prey-predator model. *Abstract and Applied Analysis* **2021** (1366797) (2021) 1–10.

[4] R. Banerjee, P. Das and D. Mukherjee. Global dynamics of a Holling Type-III two prey–one predator discrete model with optimal harvest strategy. *Nonlinear Dynamics* **99** (4) (2020) 3285-3300.

[5] B. Roy, and S. K. Roy. Prey-predator model in drainage system with migration and harvesting *Nonautonomous Dynamical Systems* **8** (1) (2021) 152–167.

[6] S. Toaha, Firman and A. Ribal. Global Stability and Optimal Harvesting of Predator-Prey Model with Holling Response Function of Type II and Harvesting in Free Area of Capture *Nonlinear Dyn. Syst. Theory* **22** (1) (2022) 105–116.

[7] K. Agnihotri and S. Nayyer. Stability Analysis of a Predator (Bird) – Prey (Fish) Harvesting Model In The Reserved and Unreserved Area *Malaya Journal of Matematik* **6** (3) (2018) 678–684.

[8] M. R. Lemnaouar, H. Benazza, M. Khalfaoui and Y. Louartassi. Dynamical behaviours of prey-predator fishery model with two reserved area for prey in the presence of toxicity and response function Holling type IV. *J. Math. Comput* **11** (3) (2021) 2893-2913.

[9] A. Pradhan, A. Johri and S. Jain. A Model for Fishery Resource with Reserve Area and Facing Prey-Predator Interaction. *International Journal of Contemporary Mathematical Sciences* **12** (6) (2017) 255–264.

[10] H. Huo, H. Jiang and X. Meng. A dynamic model for fishery resource with reserve area and taxation. *Journal of Applied Mathematics* **2012** (3) (2012) 1–15.

[11] C. Raymond, A. Hugo and M. Kung'aro. Modeling dynamics of prey-predator fishery model with harvesting: A bioeconomic model. *Journal of Applied Mathematics* **2019** (1) (2019) 1–13.

[12] N. A. Maziun and Subchan. Stability and Bifurcation Analysis of Time Delayed Prey-Predator System with Holling Type-III Response Function. *International Journal of Computing Science and Applied Mathematics* **6** (2) (2020) 59–65.

[13] F. Brauer, and C. Castillo-Chavez. *Mathematical Models in Population Biology and Epidemiology*. Second Editions. Springer, New York, 2012.

[14] B. Dubey, S. Agarwal and A. Kumar. Optimal harvesting policy of a prey–predator model with Crowley–Martin-type functional response and stage structure in the predator. *Nonlinear Analysis: Modelling and Control* **23** (4) (2018) 493–514.

[15] Didiharyono, S. Toaha, J. Kusuma and Kasbawati. Harvesting Strategies in the Migratory Prey-Predator Model with a Crowley-Martin Type Response Function and Constant Efforts *Nonlinear Dyn. Syst. Theory* **23** (1) (2023) 14–23.